Inorganica Chimica Acta 382 (2012) 146–157

Contents lists available at SciVerse ScienceDirect

Inorganica Chimica Acta

journal homepage: www.elsevier.com/locate/ica

# Copper(I)/(II) or silver(I) ions towards 2-mercaptopyrimidine: An exploration of a chemical variability with possible biological implication

G.K. Batsala [a], V. Dokorou [a,c], N. Kourkoumelis [b], M.J. Manos [d], A.J. Tasiopoulos [d], T. Mavromoustakos [e] M. Simčič [f,g], S. Golič-Grdadolnik [f,g], S.K. Hadjikakou [a,*]

[a] Section of Inorganic and Analytical Chemistry, Department of Chemistry, University of Ioannina, 45110 Ioannina, Greece
[b] Medical Physics Laboratory, Medical School, University of Ioannina, Ioannina, Greece
[c] X-ray Unit, Department of Chemistry, University of Ioannina, Ioannina, Greece
[d] Department of Chemistry, University of Cyprus, 1678 Nicosia, Cyprus
[e] Organic Chemistry Laboratory, Department of Chemistry, University of Athens, Greece
[f] Laboratory of Biomolecular Structure, National Institute of Chemistry, Hajdrihova 19, SI-1001 Ljubljana, Slovenia
[g] EN-FIST Centre of Excellence, Dunajska 156, SI-1000 Ljubljana, Slovenia

ARTICLE INFO

*Article history:*
Received 25 June 2011
Received in revised form 21 September 2011
Accepted 6 October 2011
Available online 20 October 2011

*Keywords:*
Bioinorganic chemistry
Copper(I) complexes
Silver(I) complexes
Crystal structures
Photolysis

ABSTRACT

Direct reaction of copper(I) chloride with 2-mercaptopyrimidine (pmtH) in the presence of the triphenylphosphine (tpp) in 1:1:2 M ratio forms the mixed ligand Cu(I) complex with formula $[CuCl(tpp)_2(pmtH)]$ (**1**). The dimeric $\{[Cu(tpp)(pmt)]_2$ 0.5(MeOH)$\}$ (**2**) complex was derived from the reaction of **1** with twofold molar amount of sodium hydroxide. However, the reaction of copper(II) sulfate or nitrate with pmtH and tpp in 1:2:2 M ratio, unexpectedly results in the formation of the $[CuSH(tpp)_2(pmtH)]$ (**3**) complex. Further studies have shown that the $[Cu(tpp)_2(pmt)]$ (**4**) complex is formed by reacting copper(II) acetate with pmtH in the presence of tpp in 1:2:2 M ratio, while in the absent of tpp, the $Cu(CH_3COO)_2$ or $CuSO_4$ is found to oxidizes pmtH to its corresponding disulfide $(pmt)_2$. For comparison the mixed ligand silver(I) chloride or nitrate complexes with formula $[AgCl(tpp)_2(pmtH)]$ (**5**) or $[Ag(NO_3)(tpp)_2(pmtH)]$ (**6**) are also synthesized by reacting of the AgCl or $AgNO_3$ with pmtH and tpp in 1:2:2 M ratio. The complexes have been characterized by elemental analyses, m.p., vibrational spectroscopy (mid-, far-FT-IR and Raman), $^1$H NMR, UV–Vis, ESI-MS, TG–DTA spectroscopic techniques and single crystal X-ray crystallography at ambient conditions. Photolysis of **1**–**6**, was also studied and the results showed formation of triphenylphosphine oxide. The complexes **1**–**6**, were used to study their influence upon the catalytic peroxidation of the linoleic acid by the enzyme lipoxygenase (LOX) experimentally and theoretically. The binding of **1**–**4** with LOX was also investigated by saturation transfer difference $^1$H NMR experiments (STD).



## 1. Introduction

A great number of metalloproteins and metalloenzymes such as cytochrome oxidase [1], hemocyanin [2], tyrosinase [3], etc. contain copper ions which undergo cyclic redox processes *in vivo*. Although, Cu(II) ions are usually associated with oxygen and nitrogen, and occasionally sulfur atoms of protein residues, ions of Cu(I) are likely to coordinate to sulfur containing groups. The high content of cysteine in these proteins suggests involvement of Cu(I)–sulphur interactions [4]. This led to comprehensive studies of copper ions – sulphur containing ligands, interactions [5–7]. Ottersen et al. [5a,5b] and Simmons et al. [5c] have concluded that copper(II) ions are readily reduced to copper(I) with the simultaneous oxidation of thiol ligands to the corresponding disulfides and this is also the case when copper(II) ions react with cysteine residues of proteins (Eq. (1)) [5a–c].

$$2Cu^{2+} + 2RSH \rightarrow 2Cu^{1+} + RS\text{-}SR + 2H^{+} \quad (1)$$

Wallace [5d] earlier has shown that, although disulfide was produced from the reaction between Cu(II) and thiol, however, in some cases disulfides react with cupric ions to produce sulphides [5d]. Recently, the isolation of CuS and $Cu_{1.8}S$ by reacting copper(II) with thiourea was reported [5e]. The products have been characterized with powder diffraction X-ray crystallography [5e].

Copper(I), on the other hand, is an important metal ion, which has a strong tendency to form covalent bonds with ligands containing S or P donor atoms [6,7]. Copper(I) compounds, often, forms oligomers and polymers with various coordination network types [8]. These show short Cu–Cu contacts (known as cuprophilicity) [6,7], which are less than twice the van der Waals radius of Cu

* Corresponding author. Tel.: +30 26510 08374; fax: +30 26510 08786.
*E-mail address:* shadjika@uoi.gr (S.K. Hadjikakou).

0020-1693/$ - see front matter © 2011 Elsevier B.V. All rights reserved.
doi:10.1016/j.ica.2011.10.024

(2.00–2.27 Å) [9]. Metal complexes with a $d^{10}$ configuration, in particular those containing phosphine ligands, are also known to exhibit interesting photophysical and photochemical properties [10].

Lipoxygenase (LOX) is an enzyme which catalyzes the oxidation of arachidonic acid to leukotrienes, in an essential mechanism for the cell life involving in inflammation mechanism [11a,11b]. LOX inhibition is found to induce apoptosis [11c], while the lipid peroxides derived from fatty acids metabolism by LOX can regulate cellular proliferation [11d]. Thus, LOX inhibition provides a potential novel target for the treatment and chemoprevention for a number of different cancers.

This paper, reports our studies on the structural and bioinorganic chemistry properties of $[CuCl(tpp)_2(pmtH)]$ (**1**), $\{[Cu(tpp)(pmt)]_2\ 0.5(MeOH)\}$ (**2**), $[CuSH(tpp)_2(pmtH)]$ (**3**), $[Cu(tpp)_2(pmt)]$ (**4**) and $[AgCl(tpp)_2(pmtH)]$ (**5**), $[Ag(NO_3)(tpp)_2(pmtH)]$ (**6**) complexes where pmtH = 2-mercaptopyrimidine and tpp = triphenylphosphine (Chart 1). Although the crystal structures of **1**, **4**, **6** and $(pmt)_2$ are already known [12,13], we proceed, however, their redetermination as they were needed to the understanding of the chemical behavior of the thione ligand used towards copper or silver ions.

## 2. Results and discussion

### 2.1. General aspects

Complexes **1**–**6** have been prepared as shown in Scheme 1. Crystals of complexes **1–6** and those of disulfide $(pmt)_2$ have been prepared by slow evaporation of the solutions, which remain after the filtration of the reaction solutions (Scheme 1). The crystals of complexes are air stable when they store in darkness at room temperature. The formulae of the complexes were firstly deduced from their elemental analysis, m.p., their spectroscopic data and single crystal X-ray crystallography at ambient conditions. The structures of compounds **1**, **4** and **6** are identical with those already known [12]. However, since this study aims in the elucidation of the chemical reactivity of copper(I)/(II) or silver(I) ions towards 2-mercaptopyrimidine and in the exploration of a chemical and structural variability of this interaction, we proceed their refinement here again, for comparison with those of **2**, **3** and **5**. Moreover, the structure of the disulfide $(pmt)_2$, derived from the reaction of copper acetate with 2-mercaptopyrimidine is a new polymorph and it is reported here for the first time [13]. Table 1 summarized synthetic condition, unit cell parameters and significant bond distances and angles of the already reported structures of **1**, **4**, **6** and $(pmt)_2$ [12,13].

Thus, the reaction of copper(I) chloride with 2-mercaptopyrimidine (pmtH) in the presence of triphenylphosphine (tpp) which stabilizes the + 1 oxidation state of Cu(I) ions, in 1:1:2 M ratio forms the mixed ligand Cu(I) complex of formula $[CuCl(tpp)_2(pmtH)]$ (**1**). The acidic behavior of the H(N) proton is further studied by reacting **1** with an excess sodium hydroxide which gives the dimeric $\{[Cu(tpp)(pmt)]_2\ 0.5(MeOH)\}$ (**2**) complex. In this case two [Cu(tpp)(pmt)] units come close to each other through $\mu_2$-S···Cu and N···Cu inter-unit interactions forming a dimer with strong Cu–Cu ($d^{10}$–$d^{10}$) contacts as a consequence (See also Crystal structures). However, the reaction of copper(II) sulfate or nitrate with pmtH and tpp in 1:2:2 M ratio, results in the formation of the $[CuSH(tpp)_2(pmtH)]$ (**3**) complex. The formation of **3** was detected in ESI-MS spectra by the presence of the fragments at 735.3 m/e due to the formation of $[CuSH(tpp)_2(pmtH)]^{\cdot-}$ specie towards the fragment at 734.5 m/e which corresponds to the $[CuCl(tpp)_2(pmtH)]^{\cdot-}$ in ESI-MS spectra of complexes **1**. The –SH group was identified from $\nu$(S–H) vibration band at 2640 $cm^{-1}$ in the FT-IR spectrum of **3**. The desulfuration of the thiol ligand and the formation of CuSH is also observed during irradiation of the $[\{(Ph_3P)_2Cu\}_2(dto)]$ (dto = dithioxalate) complex, where the $[(Ph_3P)_2(py)CuSH]$ complex was finally isolated [14]. In our case the CuSH could be resulted by the redox reaction between Cu(II) and pmtH [5]. However, we were unable to elucidate the fate of the pyrimidine residue although, the stoichiometry of the reaction (1:2; Cu(II):pmtH) and the reduction of Cu(II) to Cu(I) further support our assumption about the source of –SH from desulfuration of pmtH. Besides, the formation and isolation of the disulfide $(pmt)_2$, when $Cu(CH_3COO)_2$ or $CuSO_4$ reacts with pmtH further support the proposed mechanism. However, copper(II) acetate reacts with pmtH in the presence of tpp in 1:2:2 M ratio, to form the $[Cu(tpp)_2(pmt)]$ (**4**) complex, probably due to the hydrolysis of the copper(II) acetate and the basisity of the media. No desulfuration or redox reaction occurs in case the interaction between silver(I) chloride or nitrate with the same ligands. The complexes of formulae $[AgCl(tpp)_2(pmtH)]$ (**5**) or $[Ag(NO_3)(tpp)_2(pmtH)]$ (**6**) are synthesized by reacting AgCl or $AgNO_3$ with pmtH and tpp in 1:2:2 M ration.

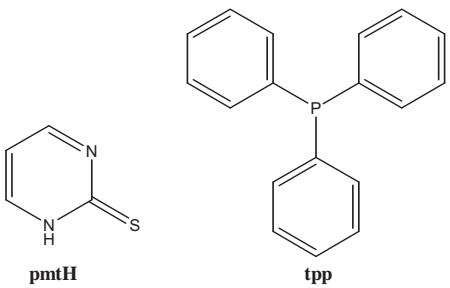


**Chart 1.** Molecular formula of 2-mercaptopyrimidine (pmyH) and triphenylphosphine (tpp).

### 2.2. Crystal structures of $\{[Cu(tpp)(pmt)]_2\ 0.5(MeOH)\}$ (**2**), $[CuSH(tpp)_2(pmtH)]$ (**3**: **3a** and **3b**) and $[AgCl(tpp)_2(pmtH)]$ (**5**) complexes

The structures of complexes **2**, **3** and **5** were determined by X-ray diffraction at 293(2) K. ORTEP diagrams of complexes **2**, **3** and **5** are shown in Figs. 1–3, while selected bond distances and angles are given in Table 2.

Complex **2** is di-nuclear with two copper ions under tetrahedral geometrical environment around each copper center. One phosphine and one deprotonated thione ligand coordinate to Cu(I) ion. The thione ligand chelates the copper(I) through N,S donor atoms. The tetrahedral coordination sphere around copper atoms consists of one P from a tpp ligand and two $\mu_2$-S and one N atoms from a deprotonated thione. Two $\mu_2$-S atoms bridge the two subunits. The Cu1–Cu1a distance is 2.6990(17) Å and is significant shorter than twofold van der Waals radius of Cu (2.00–2.27 Å) [9], indicating $d^{10}$–$d^{10}$ interaction between copper atoms [15]. Since several biological systems contain sulfur-bridged Cu(I) clusters with short Cu–Cu distances the study of such interaction is of interest [15]. This Cu···Cu distance in **2** is among the shortest found for complexes containing the $Cu_2S_2$ core (Cu–Cu varying between 2.519 and 2.888 Å (Table 3) [6a,15–17] and is also, comparable with the Cu–Cu distance in case of $Cu_8S_{12}$ bridged cluster (2.79–2.91 Å [15]).

Inter-molecular linkages, in case of **2**, via N1···C23 (solv) = 2.86(2) Å interactions (Fig. S1) lead to a polymeric assembly forming one dimensional infinite ribbon structure.

Complex **3** is monomer. Two phosphorus from two tpp ligands and one sulfur atoms from pmtH ligand are coordinated to Cu(I) cation. The tetrahedral geometry is completed by –SH group. Crystals of **3** were synthesized by reacting either $CuSO_4$ (**3a**) or

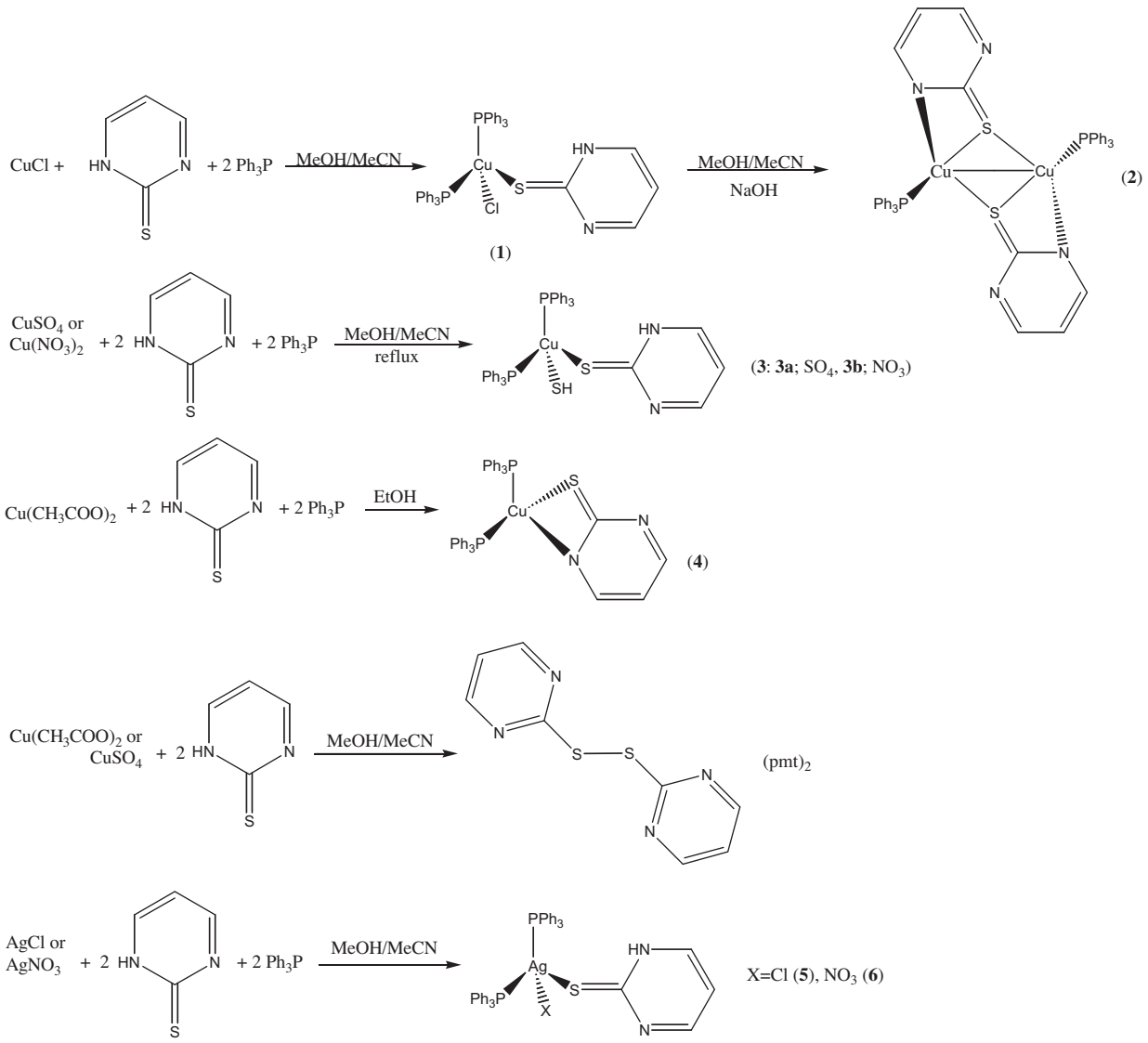


**Scheme 1.** Preparation reactions of complexes **1**–**6**.

$Cu(NO_3)_2$ (**3b**) (Scheme 1). Both complexes crystallizes in the same space group ($P2_1/c$) with identical unit cell dimensions (**3a**: $a$ = 14.4520(10), $b$ = 10.1450(10), $c$ = 24.382(2) Å, $\beta$ = 94.500(10)°, **3b**: $a$ = 14.440(4), $b$ = 10.139(3), $c$ = 24.379(4) Å, $\beta$ = 94.49(2)°). Moreover, crystals of **3a** and **3b** show similar unit cell dimension with those found for **1** (space group: $P2_1/c$, $a$ = 14.3006(3), $b$ = 10.0842(2), $c$ = 24.1240(5), $\beta$ = 94.280(2)°) indicating that the tetrahedron packet similarly in the crystal lattice in theses complexes. However, ESI-MS spectra (fragments at 735.3 and 734.5 m/e respectively corresponding to the $[CuSH(tpp)_2(pmtH)]^{\cdot -}$ and $[CuCl(tpp)_2(pmtH)]^{\cdot -}$ species) further support the formation of the CuSH from the reaction of copper(II) sulfate or nitrate with pmtH. The Cu1–S1 bond distance is 2.3652(6) Å. This is in the range of the Cu–S distance (2.322 Å) found in the $[(Ph_3P)_2(py)$-CuSH] [14]. The latter was formed by decomposition after irradiation of the complex $[\{(Ph_3P)_2Cu\}_2(dto)]$ (dto = dithioxalate).

Complex **5** is also monomer with disorder tetrahedral geometry around Ag(I) ion. Two phosphorus from two tpp ligands and one chloride atoms from pmtH ligand are coordinated to the metal center. The unit cell dimensions (14.2375(3), 10.2000(2), 24.6616(7) $\beta$ = 94.184(2)°) are close to those found for **1** and in **3a**, **3b** (see above). The Ag1–Cl1 (2.6061(4) Å), Ag1–S1 (2.6151(4) Å), Ag1–P1 (2.4647(4) Å) and Ag1–P2 (2.4572(4) Å) bond lengths are longer than the corresponding ones found in the $CuCl(tpp)_2(pmtH)$ analogue (Cu1–Cl1 = 2.3621(9), Cu1–S1 = 2.3691(10), Cu–P1 = 2.2748 (10) and Cu–P2 = 2.2852(11) Å) [12a,12b]. The bond angles around the metal center lie between 97° and 123° (Table 1) and they varied from the ideal value of 108°28′ of ideal tetrahedron due to the different strength of valance shell electron pairs repulsions (VSEPR) because of the different electronegativity of the donor atoms (P, S and Cl) bonded to Cu(I) ion.

### 2.3. Thermal decomposition

TG/DTA analysis (under nitrogen) of complexes **1** and **3**–**5** shows similar decomposition patterns. Thus, complexes **1** and **3**–**5** are stable until 200 °C and then decomposes in one endothermic step (200–300 °C) which corresponds to the mass loss of two tpp ligands (**1**: found: 77%, calc. 71%, **3**: found: 71%, calc. 71%, **4**: found: 72%, calc. 75% and **5**: found: 69%, calc. 67%). In case of **2** the TG/DTA diagram shows that the compound decomposes in two endothermic steps (130–150 and 200–250 °C), which correspond to the mass loss of two tpp (found: 31% and 40%, calc. 30%). TG/DTA diagram of **6** shows that the compound also, decomposes in two

**Table 1**
Synthetic condition, unit cell parameters and significant bond distances and angles of the reported structures for the for **1**, **4**, **5** and $(pmt)_2$.

| Complex | Unit cell | Space group | d(M–S) (Å) | d(M–P) (Å) | d(M–X) (Å) | d(C=S) (Å) | d(S···S) (Å) | Derived from | Ref. |
|---|---|---|---|---|---|---|---|---|---|
| | *a*, *b*, *c* (Å) *α*, *β*, *γ* (°) | | | | | | | | |
| 1 | 14.3006(3), 10.0842(2), 24.1240(5) 90, 94.280(2), 90 | $P2_1/c$ | 2.3691(10) M=Cu | 2.2748(10), 2.2852(11) M=Cu | 2.362 M=Cu X=Cl | 1.691 | | pmtH + CuCl + tpp MeOH/MCN | * |
| IWOSES | 14.4631(8), 10.1438(6), 24.393(1) 90, 94.564(1), 90 | $P2_1/c$ | 2.387 M=Cu | 2.290, 2.298 M=Cu | 2.366 M=Cu X=Cl | 1.679 | | pmtH + CuCl + tpp EtOH/aceton | [12a] |
| IWOSES01 | 14.340(4), 10.111(3), 24.200(5) 90, 94.363(7), 90 | $P2_1/c$ | 2.372 M=Cu | 2.290, 2.281 M=Cu | 2.368 M=Cu X=Cl | 1.691 | | pmtH + CuCl + tpp MeCN/$CHCl_3$ | [12b] |
| 4 | 9.3090(10), 11.0560(10), 18.8570(10) 93.170(10), b 91.940, 113.740(10) | $P\bar{1}$ | 2.400(2) M=Cu | 2.2413(19), 2.2560(19) M=Cu | 2.152 M=Cu X=N | 1.700 | | pmtH + $Cu(CH_3COO)_2$ + tpp EtOH | * |
| DILCAD | 9.3092(6), 11.0636(7), 18.8384(12) 93.181(1), 91.912(2), 113.810(2) | $P\bar{1}$ | 2.402 M=Cu | 2.242, 2.256 M=Cu | 2.139 M=Cu X=N | 1.716 | | pmtNa + $Cu(NO_3)_2$ MeOH/ aceton | [12c] |
| 6 | 10.0840(10), 13.5060(10), 14.310(2) 77.410(10), 78.770(10), 79.360(10) | $P\bar{1}$ | 2.5689(11) M=Ag | 2.4527(10), 2.4462(9) M=Ag | | 1.692 | | pmtH + $AgNO_3$ + tpp MeOH/ MCN | * |
| ROLVAP | 10.084(2), 13.508(3), 14.326(3) 77.43(2), 78.77(2), 79.14(2) | $P\bar{1}$ | 2.573 M=Ag | 2.447, 2.455 M=Ag | | 1.687 | | pmtH + $AgNO_3$ + tpp $CHCl_3$ | [12d] |
| $(pmt)_2$ (a) | 13.3340(3), 13.3340(3), 10.8086(4) 90, 90, 90 | $P\bar{4}2_1c$ | | | | 1.785(2), 1.787(2) | 2.0264(9) | pmtH + $Cu(MeCOO)_2$ or $CuSO_4$ MeH/MeCN | * |
| PYMDSD | 11.835(4), 6.994(1), 18.655(3) 90, 128.94(1), 90 | $P2_1/c$ | | | | 1.789,1.781 | 2.017 | pmtH water/$NH_3$ | [13a] |
| PYMDSD01 | 11.824(1), 6.9357(6), 14.4896(12) 90, 90.423(2), 90 | $P2_1/n$ | | | | 1.778, 1.781 | 2.015 | pmtH + $Bi(OH)_3$ water/$NH_3$ | [13b] |
| PYMSUL10 | 9.673(5), 15.033(6), 7.045(3) 98.73(3), 100.02(4), 86.45(4) | $P\bar{1}$ | | | | 1.1786, 1.782, 1.182, 1.777 | 2.018, 2.020 | pmtH + $Cu^{2+}$ water/$NH_3$ | [5c] |

*This work.

steps; one exothermic decomposition step between 70 and 125 °C which corresponds to the mass loss of one nitric group (found: 6%, calc. 8%) and one endothermic peak between 200 and 300 °C which corresponds to the mass loss of two tpp ligands (found: 66%, calc. 65%).

### 2.4. Continuous photolysis

Since the formation of CuSH was also observed when $[\{(Ph_3P)_2Cu\}_2(dto)]$ (dto = dithioxalate) complex irradiated by UV light to form the $[(Ph_3P)_2(py)CuSH]$ complex the continues photolysis of complexes **1**–**6** was also studied. The ultra-violet spectra of complexes **1**–**6** in chloroform are dominated by absorption bands with $\lambda_{max}$ at approximate 390, 290–260 and 240 nm respectively ($\lambda_{max}$ nm (ε); **1**: 393 (1682), 292 (12372), 240 (17257), **2**: 393 (949), 262 (20820), 240 (17231), **3**: 393 (3692), 292 (32269), 240 (31767), **4**: 393 (949), 290 (20820), 240 (17231), **5**: 393 (920), 276 (29642), 259 (30205), 240 (26793) and **6**: 364 (1748), 276 (24521), 259 (22662), 240 (23952)). Bands at app. 290–260 nm and 240 nm are ascribed to the intra-ligand ($\pi^* \leftarrow \pi$) transitions of triphenylphosphine and thione ligands [18–20], while bands at app. 390 nm are ascribed to the CT band of thione [20]. Free triphenylphosphine shows a broad band with $\lambda_{max}$ at 262 nm with a molar absorption coefficient of 11900 [20] while the spectrum of free thione in chloroform consist of absorption bands at 380.5 and 291.5 nm having ε values 1560 and 13460 respectively [20].

The light sensitivity of complexes **1**–**6** under UVC radiation was also studied. Irradiation of **1**–**6** with UVC radiation in chloroform solution at room temperature causes the decomposition of the complexes within time. Fig. 4 shows the UV spectral changes in the region of 225–400 nm of a $5 \times 10^{-5}$ M $CHCl_3$ solution of complex **2**, **3** and **5** during irradiation (0, 15, 30, 45, 60, 75, 90 and 105 s) with ultraviolet light at room temperature. In complexes **1**, **3**, **4**, **5** and **6**, a monotonic reduction of the absorbance is observed with no appearance of new bands indicating the decomposition of the complex. However, in case of **2** an increasing of the absorbance is observed initially, followed by a monotonic reduction of the absorbance. Thus, UV light, may be causes splitting of **2** to its components, which then could be decomposes similarly to the monomeric complexes **1**, **3**, **4**, **5** and **6**.

For the characterization of the photoproduct, a solution of 60 mg of complexes **1**–**6** in 10 $cm^3$ chloroform was irradiated for 1 h in a quartz conical flask under aerobic conditions. The process was monitored by TLC. The solutions were filtered off and the filtrates were concentrated to dryness. The product generated in all cases was verified from its physical (m.p. = 149–151 °C) and spectral (FT-IR) data which are identical with the corresponding data of triphenylphoshine oxide [18]. Fig. 5 shows the FT-IR spectrum of complex **3** (**A**) and the correspondiong of its photoproduct derived upon continues photolysis of **3** (**B**) in contrast to the spectrum of triphenylphoshine oxide (**C**). The presence of the $\nu$(P=O) vibration band at 1376 $cm^{-1}$ in the IR spectra of the complexes indicates the phosphine oxide formation [18]. Reva et al. have previously concluded that irradiation of tpp with UV light in the presence of oxygen lead to the formation of triphenylphoshine oxide [21]. Therefore, based on these findings, tpp ligand is released in solutions of **1** and **2** during photolysis which followed by its oxidation to triphenylphoshine oxide by air.

### 2.5. Study of the peroxidation of linoleic acid with the enzyme lipoxygenase in the presence of complexes *1*–*6*

In order to investigate the modification in an enzyme activity caused by the copper or silver complexes the influence of complexes **1**–**6** on the oxidation of linoleic acid by lipoxygenase was studied in a wide concentration interval. The activity of the

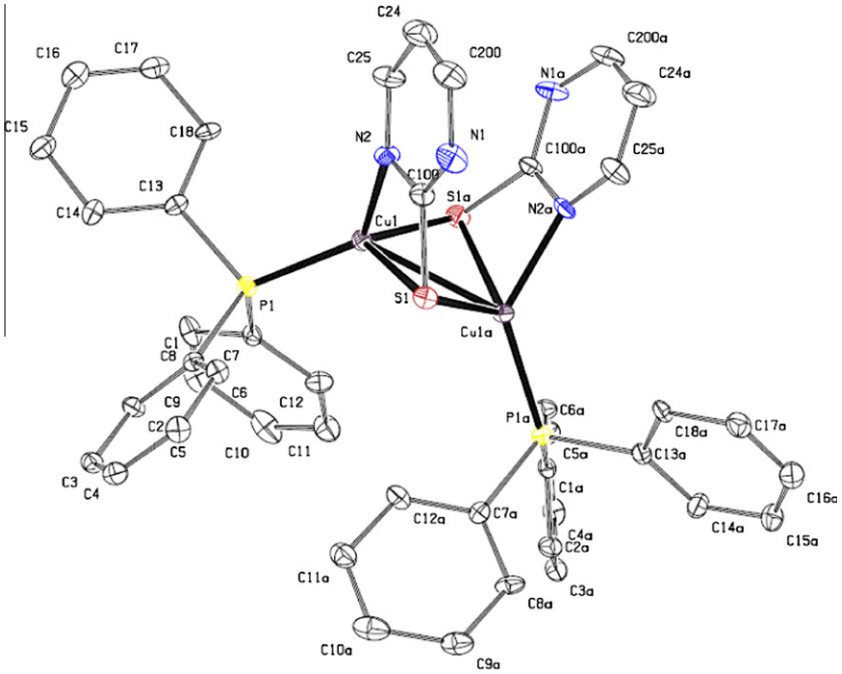


**Fig. 1.** (A) ORTEP diagram of compound **2** together with the atomic numbering scheme. Thermal ellipsoids drawn at the 50% probability level. Solvent molecule is omitted for clarity.

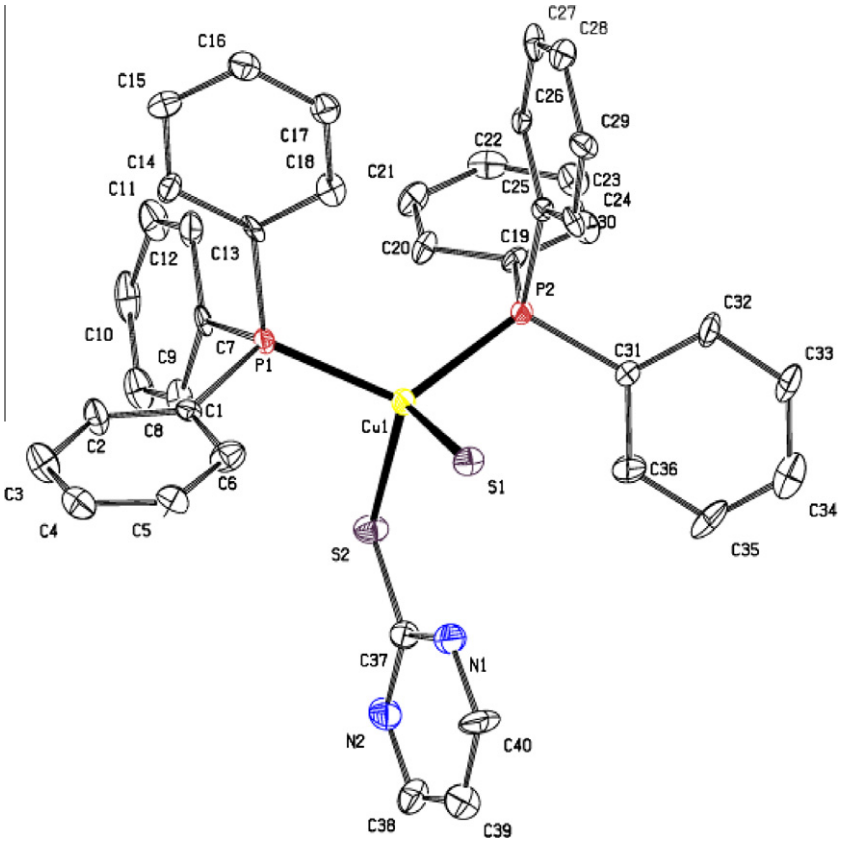


**Fig. 2.** ORTEP diagram of compound **3** together with the atomic numbering scheme. Thermal ellipsoids drawn at the 50% probability level.

enzyme (*A*, %) in the presence of the complex was calculated using a known procedure [22a]. The concentrations at which the enzymatic activity is inhibited by 50% ($IC_{50}$) for the complexes are: 24 (**1**), 7 (**2**), 30 (**3**), 19 (**4**), 28 (**5**) and 47 (**6**) μM, respectively, Thus the dimmer complex **2** showed the strongest inhibitory activity among the compounds tested.

The binding of **1**, **2**, **3** and **4** towards LOX was also investigated by saturation transfer difference $^1$H NMR experiment. On the top of

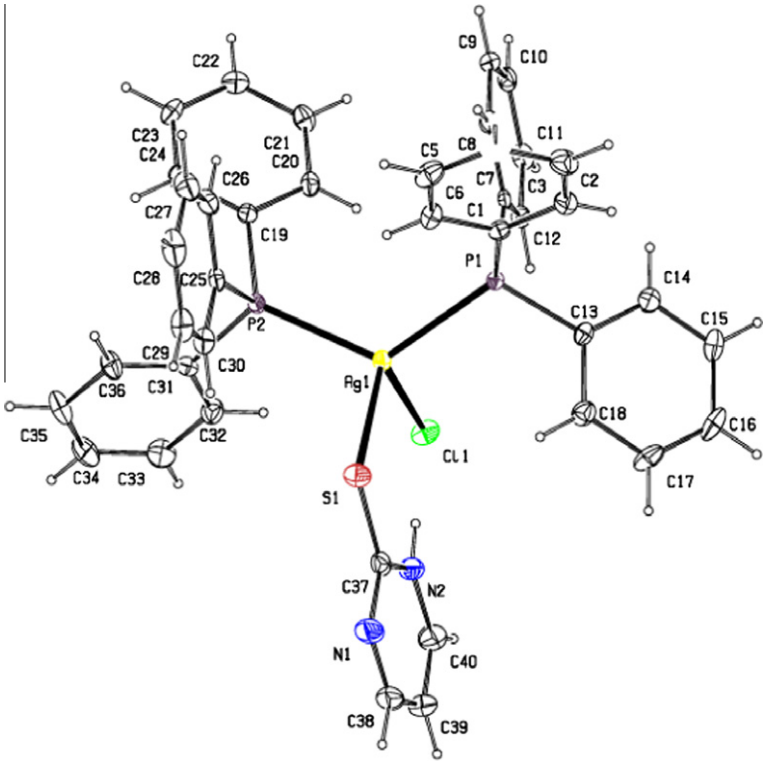


**Fig. 3.** ORTEP diagram of compound **5** together with the atomic numbering scheme. Thermal ellipsoids drawn at the 50% probability level.

**Table 2**
Selected bond lengths (Å) and angles (°) of complexes **2**, **3** and **5**.

| Complex **2** | | Complex **3a** | | Complex **3b** | | Complex **5** | |
|---|---|---|---|---|---|---|---|
| *(a) Bond lengths* | | *(a) Bond lengths* | | *(a) Bond lengths* | | | |
| Cu1–S1 | 2.671(3) | Cu1–S1 | 2.3652(6) | Cu1–S1 | 2.3629(6) | Ag1–Cl1 | 2.6061(4) |
| Cu1–P1 | 2.198(2) | Cu1–S2 | 2.3718(5) | Cu1–S2 | 2.3697(5) | Ag1–S1 | 2.6151(4) |
| Cu1–N2 | 2.051(7) | Cu1–P1 | 2.2861(6) | Cu1–P1 | 2.2842(6) | Ag1–P1 | 2.4647(4) |
| Cu1–S1a | 2.313(3) | Cu1–P2 | 2.2770(5) | Cu1–P2 | 2.2735(5) | Ag1–P2 | 2.4572(4) |
| Cu1–Cu1a | 2.6990(17) | S1–C37 | 1.692(2) | S1–C37 | 1.687(2) | S1–C37 | 1.6913(16) |
| S1–C9 | 1.734(10) | | | | | | |
| *(b) Angles* | | *(b) Angles* | | *(b) Angles* | | | |
| S1–Cu1–P1 | 119.62(9) | S1–Cu1–S2 | 108.69(2) | S1–Cu1–S2 | 108.76(2) | Cl1–Ag1–S1 | 103.56(1) |
| S1–Cu1–N2 | 65.7(3) | S1–Cu1–P1 | 98.03(2) | S1–Cu1–P1 | 97.94(2) | Cl1–Ag1–P1 | 98.43(1) |
| Cu1a–Cu1–S1 | 51.02(7) | S1–Cu1–P2 | 111.87(2) | S1–Cu1–P2 | 111.85(2) | Cl1–Ag1–P2 | 110.80(1) |
| S1–Cu1–S1a | 111.67(9) | S2–Cu1–P1 | 113.85(2) | S2–Cu1–P1 | 113.97(2) | S1–Ag1–P1 | 116.61(1) |
| Cu1a–S1–Cu1 | 65.11(7) | S2–Cu1–P2 | 102.33(2) | S2–Cu1–P2 | 102.23(2) | S1–Ag1–P2 | 102.71(1) |
| | | P1–Cu1–P2 | 121.87(2) | P1–Cu1–P2 | 121.90(2) | P1–Ag1–P2 | 123.18(1) |

Fig. 6A–D the aromatic region of the off-resonance NMR spectra are shown and on the bottom the on-resonance saturation transfer difference $^1$H NMR spectra of the complexes **1**, **2**, **3** and **4**. Resonance signals attributed to the aromatic protons of the ligands *ca* 7.8–7.5 ppm of the complexes studied are present in the binding mode of the protein. Signals at 7.5–7.65 ppm are attributed to triphenylphosphine, while those at 7.7–7.8 ppm to 2-mercaptopyrimidine. Thus, both components of the complexes, pmtH and triphenylphosphine have binding affinity at LOX receptor [22b]. This experiment provides direct evidence for the binding affinity of the complexes with LOX and supports experimental results reported above.

### 2.6. Computational studies

Molecular docking studies have been used to further assess the inhibitory effectiveness of the complexes on LOX. There does not seem to be any preferable binding pocket for all the complexes indicating different interaction relationships towards the enzyme inhibition. Close values of binding energy are perceived even for completely different poses and binding orientations. Since the results might be misleading regarding the topological parameters, our conclusions are based on the total binding energy of the inhibitors and substrate. The binding energy ($E$) of the substrate (S: linoleic acid) to its binding site in the enzyme LOX (**E**) when **ES** (enzyme:substrate) complex formed, is $E = -100.2$ kJ/mol. The corresponding binding energies of inhibitors (**I**), in **EI** (enzyme:inhibitor) and **ESI** (enzyme:substrate:inhibitor) are calculated and shown along with the experimental $IC_{50}$ values in Table 4.

The complexes with the lowest **EI** (**1**, **2**, **3**, **5**) reside to the active site of the protein as this was identified by our group [23] while their energy is higher than that of the **ES**. It is noteworthy to mention that among amino acid residues which form the docking cavity of the inhibitor **1**, **2**, **3** and **5** in EI complex, cysteine is included

**Table 3**
Reported copper–copper (Å) distances in complexes.

| Complex | | (Cu···Cu) (Å) | Ref. |
|---|---|---|---|
| $\{[Cu(tpp)(pmt)]\ 0.5(MeOH)\}_2$ | **2** | 2.6990(17) | * |
| $[Cu_2L(SCN)_2]$ | AZFRCU | 2.796 | [16a] |
| $Cu(tu)_3BF_4$ | CUDMTB20 | 2.840(3) | [16b] |
| $Cu(S\text{-}dmtu)_3BF_4$ | CUTUBF30 | 2.828 | [16b] |
| $[CuSCN(pytH)_2]_2$ | EGEWIW | 2.888 | [16c] |
| $[Cu(C_9H_6NS)]_n$ | EKALIL | 2.7922(8) | [16d] |
| $[Cu_2(MePh\text{-}mpt)_2(PPh_3)_2]$ | FOSTOX | 2.845(1) | [16e] |
| $[Cu(SC_6H_4CH_3\text{-}o)(l,l0\text{-phenanthroline}]_2\ CH_3CN$ | FULXOZ | 2.613(3) | [16f] |
| $\{[Cu_2(bzimztH)_5]\}_2(ClO_4)_2\ 7H_2O$ | GEZWOX | 2.681(2) | [16g] |
| $[Cu_4(\mu_2\text{-dppm})_3(\mu_2\text{-}\mu_2\text{-}NS_2)(\mu_2\text{-}\mu_2\text{-}NS_2)]$ | | 2.641(2) | [16h] |
| $[Cu(tmtp)(bzimtH)Cl]_2$ | KUTSIB | 2.764(l) | [6a] |
| [Cu(siig)(pp)] | LAZLUT | 2.797(3) | [17a] |
| $[Cu_7(StBu)_4(hfa)_3(PMe_3)_3]$ | MECZUQ | 2.519 | [17b] |
| $\{[Cu^{I}_{10}Cu^{II}_2(MMI)_{12}(MeCN)_4](BPh_4)(MeCN)_4\}$ | MRIMCU | 2.547(1) | [17c] |
| $[Cu_6(dmpymt)_6]$ | PAKSOJ | 2.759(2) | [17d] |
| $[Cu_2\{\mu\text{-}SC(NH_2)_2\}_2\{SC(NH_2)_2\}_4]^{2+}$ | PUTRIF | 2.5526(5) | [17e] |
| $[Au^{III}Cu^{I}_8(\mu\text{-dppm})_3(tdt)_5]^{+}$ | TAVYIZ | 2.701(5) | [17f] |
| $[Cu(bztzdtH)(PPh3)Br]_2$ | TAZHEH | 2.928(1) | [16g] |

*This work, L = 20-membered macrocyclic Schiff base, tu = thiourea, S-dmtu dimethylthiourea, pytH = 2-mercaptopyridine, $C_9H_6NS$ = 8-thioquinoline, MePh-mpt = methylphenylpyruvate thiosemicarbazone, $PPh_3$ = triphenylphosphine, $HSC_6H_4CH_3$-o = o-tolylthiole, bzimztH = 2-mercaptobenzimidazole, dppm = bis-(diphenylphoshino) methane, $NS_2^{2-}$ = 1,8-naphthalenedithiolate, tmtp = tris(m-tolyl)phosphine, bzimtH = benzimidazole-2-thione, Hsiig = 1,2:5,6-di-*O*-isopropylidene-3-thio-a-o-glucofuranose, pp = 1,2-bis(diphenylphosphinoethene), hfa = hexafluoroacetylacetonate, MMI = N-methyl-2-mercaptoimidazole, Hdmpymt = 4,6-dimethylpyrimidine-2-thione, tdt = toluene-3,4-dithiolate, dppm = bis(diphenylphosphino)methane, bztzdtH = benz-1, 3-thiazolidine-2-thione.

(Table 4). When the substrate is present, all molecules bind away to another pocket which is thermodynamically far more favorable for **1**, **2**, **3** and **5** than the **EI** analogous and comparable to the **EI** complex in the case of **4** and **6**. The stability of the **ESI** complexes features a positive correlation with the inhibitory effect evaluated experimentally although this finding is probably coincidental since the effectiveness of irreversible inhibitors cannot be assessed by $IC_{50}$ values.

## 3. Conclusions

The complexes **1**–**6** were studied here for their structural, photochemical and bioinorganic properties. 2-Mercaptopyrimidine is readily coordinated to copper(I) chloride in the presence of tpp to form the monomer complex $[CuCl(tpp)_2(pmtH)]$ (**1**). This is also the case when silver chloride and nitrate is used, where the $[AgCl(tpp)_2(pmtH)]$ (**5**) or $[Ag(NO_3)(tpp)_2(pmtH)]$ (**6**) complexes are formed. The acidic behavior of the H(N) proton in **1** was proved by the formation of the dimeric $\{[Cu(tpp)(pmt)]\ 0.5(MeOH)\}_2$ (**2**) complex when **1** reacts with sodium hydroxide. In this case two [Cu(tpp)(pmt)] units come close to form the dimer due to strong $\mu_2$-S and N–Cu inter-unit interactions with Cu–Cu ($d^{10}$–$d^{10}$) contacts as a consequence. The Cu···Cu distance of 2.700(2) Å in **2**, is significant shorter from the twofold of copper Waals radius (4.00–4.54 Å) [3]. Therefore this distance could be defined as Cu–Cu bonding interaction.

The reaction of copper(II) sulfate or nitrate with pmtH and tpp, on the other hand, results in the formation of the $[CuSH(tpp)_2(pmtH)]$ (**3**) complex. The formation CuSH could be explained by the redox reaction between Cu(II) and pmtH [5] (Scheme 2). Besides, the formation of the disulfide $(pmt)_2$, when $Cu(CH_3COO)_2$ or $CuSO_4$ reacts with pmtH further support the proposed reaction path.

Irradiation of **1**–**6** with UVC light caused their decomposition and the formation of triphenylphosphine oxide. In contrary, to the formation of CuSH which derived during irradiation of the $[\{(Ph_3P)_2Cu\}_2(dto)]$ (dto = dithioxalate) complex [14], no any deposition of CuSH, by desulfuration of the thiole ligand, was observed in the case of **1**–**6** complexes.

Spectroscopic data (UV and NMR) show that complexes **1**–**6**, inhibit the catalytic peroxidation of linoleic acid by the enzyme LOX. Docking calculations also show that among amino acid residues which form the docking cavity of the inhibitor **1**, **2**, **3** and **5** in EI complex, cysteine is included (Table 4). Since sulfur containing amino acids, such as cysteine, are known to play an important role on the proteins function by stabilizing their intermolecular assemblies thought –SH hydrogen bonding interactions or –S–S– bonds, the desulfuration of the thiols upon redox reaction with copper(II) salts might be modulating protein activity.

## 4. Experimental

### 4.1. Materials and instruments

All solvents used were reagent grade. Copper(I) chloride (Riedel–deHaen), triphenylphosphine (Merk) ligand (Aldrich-Merk) were used with no other purification prior to use. Elemental analyses for C, H, N, and S were carried out with a Carlo Erba EA MODEL 1108. Melting points were measured in open tubes with a STUART scientific apparatus and are uncorrected. Infra-red spectra in the region of 4000–370 $cm^{-1}$ were obtain in KBr discs while far-infra-red spectra in the region of 400–50 $cm^{-1}$ were obtain in polyethylene discs, with a Perkin-Elmer Spectrum GX FT-IR spectrometer. A Jasco UV/Vis/NIR V 570 series spectrophotometer was used to obtain the electronic absorption spectra. Thermal studies were carried out on a Shimadzu DTG-60 simultaneous DTA–TG apparatus, under a $N_2$ flow (50 $cm^3\ min^{-1}$) at a heating rate of 10 °C $min^{-1}$.

### 4.2. Synthesis and crystallization of $[CuCl(tpp)_2(pmtH)]$ (**1**), $\{[Cu(tpp)(pmt)]_2\ 0.5(MeOH)\}$ (**2**), $[CuSH(tpp)_2(pmtH)]$ (**3**), $[Cu(tpp)_2(pmt)]$ (**4**), $[AgCl(tpp)_2(pmtH)]$ (**5**) and $[Ag(NO_3)(tpp)_2(pmtH)]$ (**6**) complexes

The synthesis and characterization of **1**, **4**, **6** and $(pmt)_2$ are already reported [12,13]. However, these compounds and the complexes **2**, **3** and **5** were prepared also here as follows: 1 mmol (0.262 g) triphenylphosphine and 0.5 mmol (0.056 g)

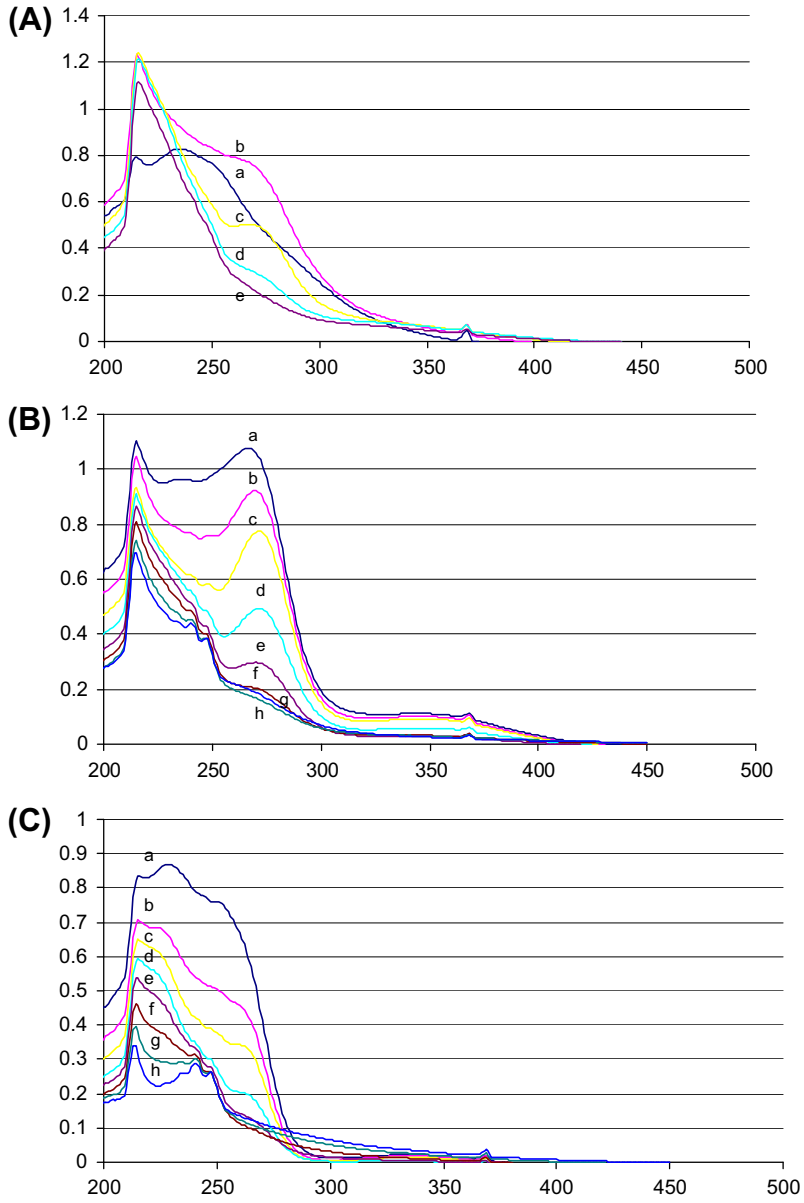


**Fig. 4.** UV absorption spectrum of $5 \times 10^{-5}$ M $CHCl_3$ solution containing **2** (**A**), **3** (**B**) or **5** (**C**), after irradiation with UVC light at room temperature for 0 (a), 15 (b), 30 (c), 45 (d), 60 (e), 75 (f), 90 (g) and 105 (h) s.

2-mercaptoryrimidine were suspended to 20 $cm^3$ methanol/acetonitrile solution (1:1) which contains 0.5 mmol of copper(I) chloride (0.052 g) (**1**), silver chloride (0.072 g) (**5**) or silver nitrate (0.085 g) (**6**). The mixture was stirred until a clear solution is formed. The clear solution was then filtered off and kept in darkness at r.t. After 24 h orange (**1**) or yellow (**5**, **6**), crystals, of complexes suitable for single crystal analysis by X-ray crystallography, were filter off.

Methanol solution (10 $cm^3$) of 2 mmol NaOH (0.008 g) was added to a suspension of 20 $cm^3$ methanol/acetonitrile (1:1) which contains 1 mmol $[CuCl(tpp)_2(pmtH)]$ (0.074 g) and the solution was stirred, until a clear solution is formed. The solution was filtered off and it kept in darkness at r.t. Few days after, yellow crystals of **2**, suitable for single crystal analysis by X-ray crystallography were filter off.

A suspension of 0.5 mmol copper(II) sulfate pentahydrate (0.124) g or copper(II) nitrate trihydrate (0.121 g), 1 mmol triphenylphosphine (0.262 g) and 1 mmol 2-mercaptoryrimidine (0.112 g) in 20 $cm^3$ methanol/acetonitrile (1:1) is heated under reflux, until a clear solution. The solution was filtered off and the clear solution was kept in darkness at r.t. After few days orange crystals, of complex **3** suitable for single crystal analysis by X-ray crystallography, was filter off.

Copper(II) acetate1-hydrate, (0.5 mmol, 0.263 g), triphenylphosphine (1 mmol, 0.262 g) and 2-mercaptoryrimidine (1 mmol, 0.113 g) are suspended in 15 $cm^3$ ethanol. The mixture is stirred until a clear solution is formed. The solution was then filtered off and it kept in darkness at r.t. After few days, light orange crystals, of complex **4** suitable for single crystal analysis by X-ray crystallography, was filter off. The disulfite of 2-mercaptopyrimidiner was prepared as follows: copper(II) acetate1-hydrate, (0.5 mmol, 0.263 g) and 2-mercaptoryrimidine (1 mmol, 0.113 g) were dissolved in 20 ml methanol/acetonitrile (1:1). The clear solution was filtered off and it was kept in darkness at r.t. After few days pale orange crystals, of $(pmt)_2$ suitable for single crystal analysis by X-ray crystallography, was filter off.

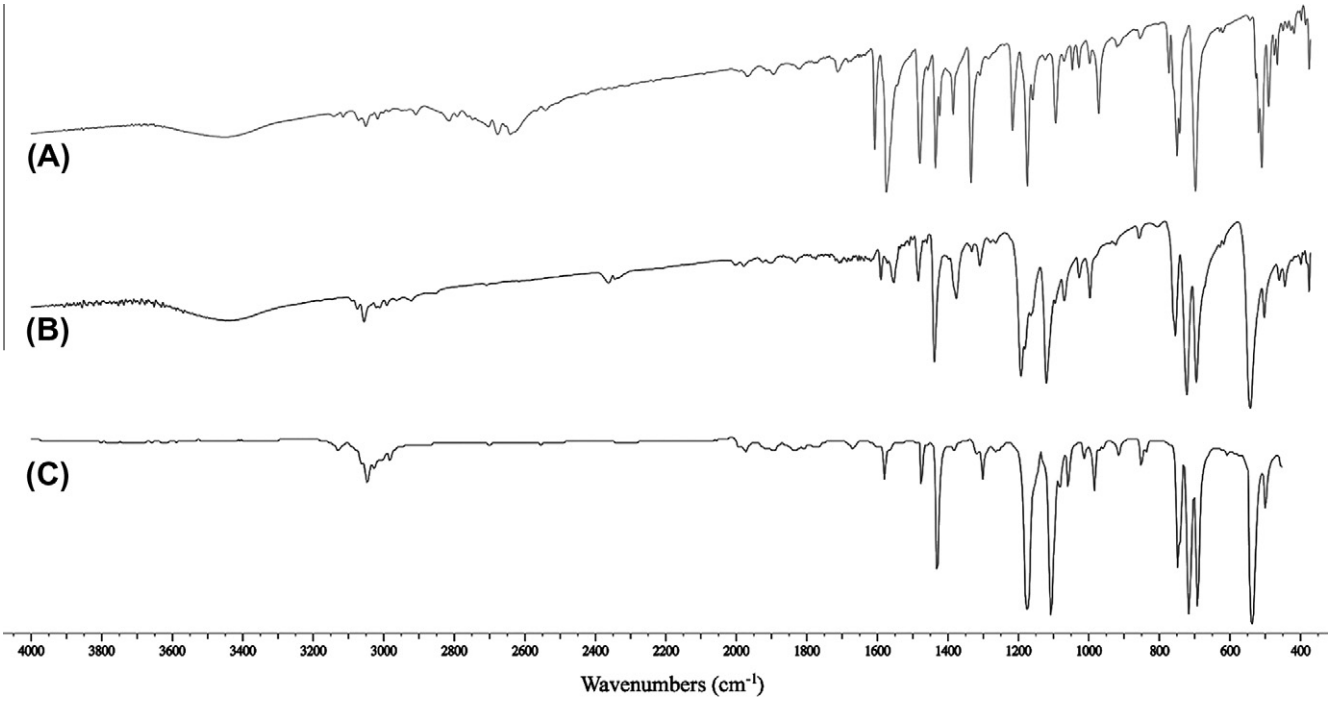


**Fig. 5.** FT-IR spectrum of complex **3** (**A**) and its photoproduct derived upon continues photolysis of 3 (**B**) in contrast to the corresponding spectrum of triphenylphoshine oxide (**C**).

Complex **1**: orange crystal, yield: 80%, melting point: 193–197 °C. Elemental analysis, *Anal.* Calc. for $C_{40}H_{34}ClCuN_2P_2S$: C, 65.3; H, 4.55; N, 3.81; S, 4.36. Found: C, 65.7; H, 4.67; N, 3.34; S, 4.88%. IR ($cm^{-1}$), (KBr): 1608vs, 1434s, 1174s, 997m, 517s; Far-IR ($cm^{-1}$), (polyethylene): 241m, 205m, 120vs; MS *m*/*z*: 735.5 $[CuCl(tpp)_2(pmtH)]^{-}$, 587 $[Cu(tpp)_2]^{+}$; UV–Vis ($CHCl_3$): $\lambda_{max}$ ($\log\varepsilon$): 392 nm (3.22), 291 nm (4.09), 239 nm (4.24); Raman ($cm^{-1}$): 207s, 414 m, 441 m.

Complex **2**: yellow crystal, yield: 10%, melting point: >260 °C. Elemental analysis, *Anal.* Calc. for $C_{44}H_{36}Cu_2N_4P_2S_2$: C, 60.47; H, 4.15; N, 6.41; S, 7.34. Found: C, 59.4; H, 4.25; N, 6.50, S, 7.55%. IR ($cm^{-1}$), (KBr): 1567s, 1377vs, 1178s, 1094m, 504s; Far-IR ($cm^{-1}$), (polyethylene): 225vs, 210s, 125 ms; MS *m*/*z*: 808 $[Cu(tpp)_2(pmtH)_2]^{+}$, 587 $[Cu(tpp)_2]^{+}$; UV–Vis ($CHCl_3$): $\lambda_{max}$ ($\log\varepsilon$): 392 nm (2.98), 261 nm (4.32), 239 nm (4.24); Raman ($cm^{-1}$): 123m, 320m, 418s, 440m.

Complex **3**: orange crystal, yield: 10% (15% when copper(II) nitrate trihydrate was used), melting point: 194–199 °C. Elemental analysis, *Anal.* Calc. for $C_{40}H_{35}CuN_2P_2S_2$: C, 65.52; H, 4.81; N, 3.82; S, 8.74. Found: C, 65.45; H, 4.62; N, 3.41; S, 8.44%. IR ($cm^{-1}$), (KBr): 1607m, 1575vs, 1175s, 1094m, 508s; Far-IR ($cm^{-1}$), (polyethylene): 205m, 123m; MS *m*/*z*: 734.6 $[CuSH(tpp)_2(pmtH)]^{-}$, 587 $[Cu(tpp)_2]^{+}$; UV–Vis ($CHCl_3$): $\lambda_{max}$ ($\log\varepsilon$): 392 nm (3.57), 291 nm (4.50), 239 nm (4.50); Raman ($cm^{-1}$): 414s, 444m.

Complex **4**: light orange crystal, yield: 42%, melting point: 153–157 °C. Elemental analysis, *Anal.* Calc. for $C_{40}H_{33}CuN_2P_2S$: C, 68.71; H, 4.75; N, 4.01; S, 4.58. Found: C, 69.10; H, 4.35; N, 3.90; S, 4.92%. IR ($cm^{-1}$), (KBr): 1567s, 1370vs, 1181 ms, 1094s, 516s; Far-IR ($cm^{-1}$), (polyethylene): 221 m, 205m, 124s; MS *m*/*z*: 587 $[Cu(tpp)_2]^{+}$; UV–Vis ($CHCl_3$) $\lambda_{max}$ ($\log\varepsilon$): 392 nm (3.12), 261 nm (4.45), 239 nm (4.37); Raman ($cm^{-1}$): 350m, 418s, 435m.

Complex **5**: yellow crystal, yield: 74%, melting point: 175–180 °C. Elemental analysis, *Anal.* Calc. for $C_{40}H_{34}ClAgN_2P_2S$: C, 61.59; H, 4.39; N, 3.59; S, 4.11. Found: C, H, N. IR ($cm^{-1}$), (KBr): 1608s, 1435s, 1175s, 1095m, 506s; Far-IR ($cm^{-1}$), (polyethylene): 247m, 191m, 139vs; MS *m*/*z*: 631 $[Ag(tpp)_2]^{+}$, UV–Vis ($CHCl_3$): $\lambda_{max}$ ($\log\varepsilon$): 392 nm (2.96), 275 nm (4.47), 258 nm (4.48), 240 nm (4.43); Raman ($cm^{-1}$): 171 m, 210 m, 319 m.

Complex **6**: yellow crystal, yield: 86%, melting point: 155–160 °C. Elemental analysis, *Anal.* Calc. for $C_{40}H_{34}AgN_3O_3P_2S$: C, 59.57; H, 4.24; N, 5.21; S, 3.97. Found: C, 59.90; H, 4.21; N, 5.00; S, 4.10. IR ($cm^{-1}$), (KBr): 1608vs, 1478s, 1186s, 984m, 506s; Far-IR ($cm^{-1}$), (polyethylene): 247m, 191m, 139vs; MS *m*/*z*: 851 $[Ag(tpp)_2]^{+}$, UV–Vis ($CHCl_3$): $\lambda_{max}$ ($\log\varepsilon$): 393 nm (3.13), 278 nm (4.15), 239 nm (4.19); Raman ($cm^{-1}$): 126m, 179m, 324m.

### 4.3. X-ray structure determination

Intensity data for the crystals of **1**, **3** and **5** were collected on an Oxford Diffraction CCD instrument [24a], while a Bruker P4 diffractometer was used for **2**, **4** and **6** using graphite-monochromated Mo radiation ($\lambda$ = 0.71073 Å). Cell parameters were determined by least-squares refinement of the diffraction data from 25 reflections [24b,24c].

All data were corrected for Lorentz-polarization effects and absorption [24a,24b]. The structures were solved with direct methods with SHELXS97 [24c] and refined by full-matrix least-squares procedures on $F^2$ with SHELXL-97 [24d] All non-hydrogen atoms were refined anisotropically, hydrogen atoms were located at calculated positions and refined via the "riding model" with isotropic thermal parameters fixed at 1.2 (1.3 for $CH_3$ groups) times the $U_{eq}$ value of the appropriate carrier atom. Significant crystal data for the structure **2**, **3a**, **3b**, **5** and $(pmt)_2$ are given in Table 5.

### 4.4. Photolysis studies

A TUV 15W G15 T8 low-pressure mercury vapour discharge lamps with a tubular glass envelope UVC lamp, 15 watt, manufactured by Phillips was used for the photolysis. The photolysis was performed as follows: A $5 \times 10^{-5}$ M solution of **1**–**6** in chloroform

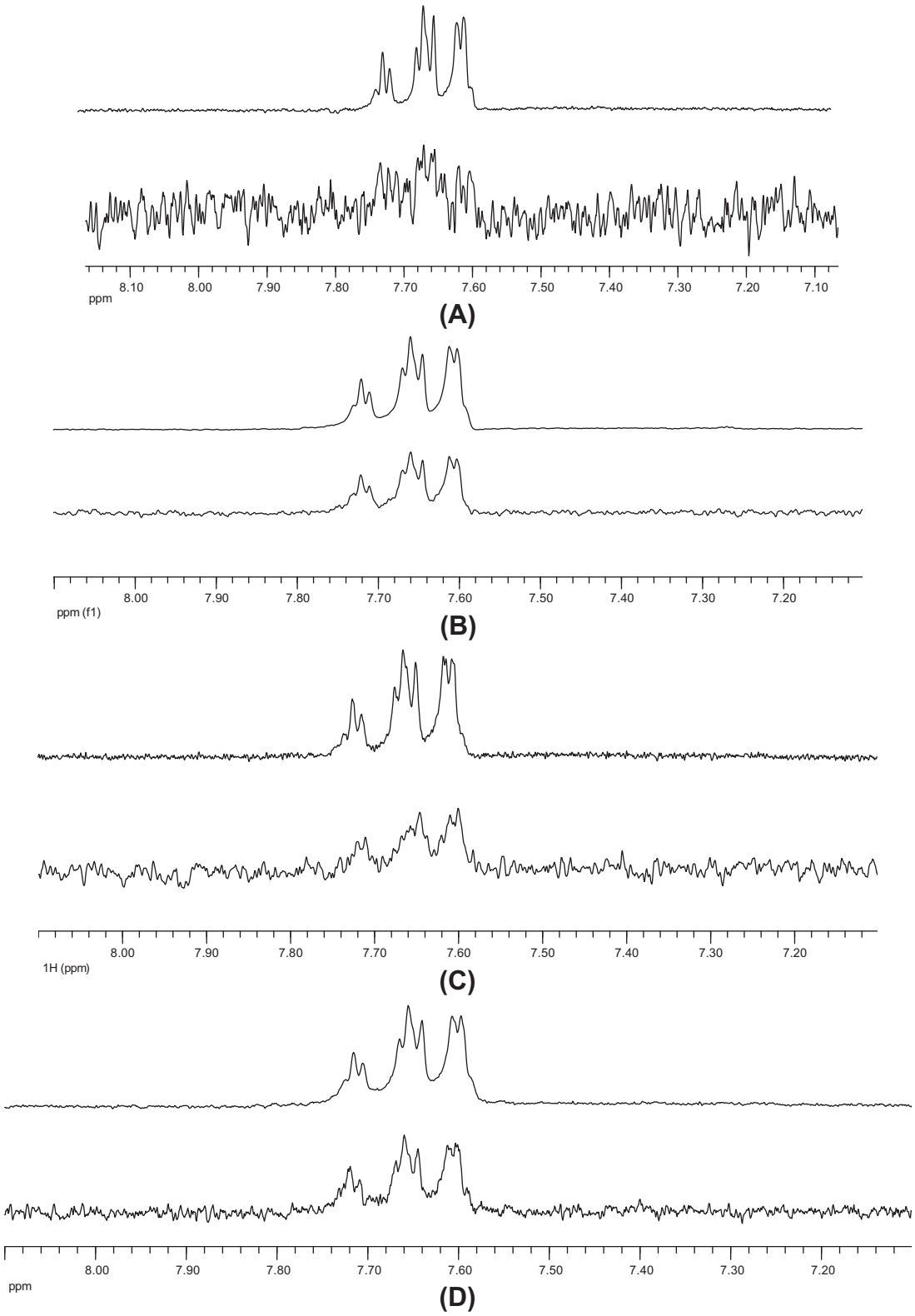


**Fig. 6.** Off-resonance reference NMR spectrum (top) and on-resonance saturation transfer difference NMR spectrum (bottom) for the **1** (**A**), **2** (**B**), **3** (**C**) and **4** (**D**) complexes. Spectra are not to scale, on-resonance saturation transfer difference NMR spectrum has approximately 200-fold (**1**), 50-fold (**2**), 60-fold (**3**) and 25-fold (**3**) lower intensity compared to the corresponding reference spectra.

was kept in a 1 cm quartz cell under aerobic conditions and the solution was irradiated with ultraviolet light (all spectrum). The cell was placed at a distance of 20 cm from the UV source. Characterization of the photo-products was carried out on a solution of 0.060 g of **1**–**6** in 10 $cm^3$ chloroform which was irradiated for 1 h in a quartz conical flask under aerobic conditions.

**Table 4**
Binding energies of inhibitors (**I**), in enzyme:inhibitor (**EI**) and enzyme:substrate:inhibitor (**ESI**) complexes along with the experimental $IC_{50}$ values.

| Complexes | **EI** (kJ/mol) | **ESI** (kJ/mol) | Amino acid residues form the docking cavity of the inhibitor in EI complex | $IC_{50}$ (μM) |
|---|---|---|---|---|
| **1** | −64.9 | −95.0 | Arg533, Arg767, Asn128, Asn534, Asn535, Asn769, Asn835, Asp243, Asp768, Cys127, Gln766, Glu244, His515, His531, Leu246, Leu527, Lys526, Phe108, Pro530, Ser129, Thr529, Trp772, Tyr184, Tyr525, Tyr532, Val126, Val520, Val762 | 24 |
| **2** | −40.35 | −98.8 | Ala145, Arg141, Arg182, Arg533, Arg767, Asn128, Asn146, Asn534, Asn769, Asp243, Asp768, Cys127, Glu244, His515, His522, Leu169, Leu246, Leu527, Lys526, Phe108, Phe143, Phe144, Pro530, Ser129, Thr529, Trp772, Tyr184, Tyr525, Tyr532, Val126, Val520 | 7 |
| **3** | −69.7 | −87.6 | Arg533, Arg767, Asn128, Asn534, Asn769, Asn835, Asp243, Asp768, Cys127, Glu244, His515, Leu246, Lys110, Lys526, Phe108, Pro530, Thr529, Trp772, Tyr525, Tyr532, Val126, Val520, Val762 | 30 |
| **4** | −98.1 | −100.8 | Ala426, Ala710, Arg712, Asn424, Asn550, Gln267, Glu271, Glu282, Glu554, Ile281, Ile738, Ile746, Leu423, Leu558, Leu742, Lys741, Phe274, Phe557, Pro559, Pro743, Ser425, Ser560, Ser740, Thr555, Thr556, Thr709, Thr739 | 19 |
| **5** | −19.5 | −97.1 | Arg141, Arg182, Arg533, Arg767, Asn128, Asn534, Asn769, Asn835, Asp243, Asp768, Cys127, Glu244, His515, His531, Leu246, Leu527, Lys526, Phe108, Phe143, Phe144, Pro530, Ser129, Thr529, Trp772, Tyr525, Tyr532, Val126, Val520, Val762 | 28 |
| **6** | −98.9 | −85.0 | Arg318, Gln329, Gln334, Glu315, Glu752, Gly827, His331, Leu316, Leu828, Lys326, Phe327, Pro328, Pro330, Pro699, Thr756, Thr829, Tyr293, Tyr317, Tyr698 | 47 |

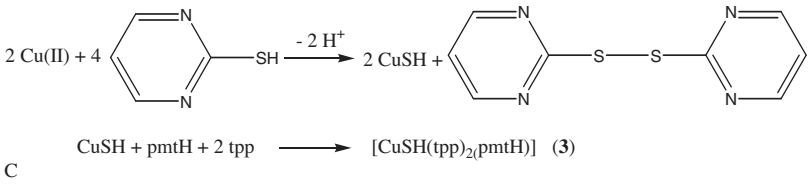


**Scheme 2.**

**Table 5**
Structure refinement details for the complexes **3–7**.

| | **2** | **3a** | **3b** | **5** | $(pmt)_2$ |
|---|---|---|---|---|---|
| Empirical formula | $C_{44}H_{36}Cu_2N_4P_2S_2$ 0.5($CH_3OH$) | $C_{40}H_{34}CuN_2P_2S_2$ | $C_{40}H_{34}CuN_2P_2S_2$ | $C_{40}H_{34}AgClN_2P2S$ | $C_8H_6N_4S_2$ |
| Formula weight | 896.52 | 732.32 | 732.32 | 780.02 | 222.31 |
| $T$ (K) | 293(2) | 293(2) | 293(2) | 293(2) | 293(2) |
| Crystal system | orthorhombic | monoclinic | monoclinic | monoclinic | tetragonal |
| Space group | *Pbcn* | $P2_1/c$ | $P2_1/c$ | $P2_1/c$ | $P\bar{4}2_1c$ |
| $a$ (Å) | 19.171(4) | 14.3078(3) | 14.2936(4) | 14.2375(3) | 13.3340(3) |
| $b$ (Å) | 11.667(2) | 10.0923(2) | 10.0800(2) | 10.2000(2) | 13.3340(3) |
| $c$ (Å) | 18.729(3) | 24.1358(4) | 24.1214(6) | 24.6616(7) | 10.8086(4) |
| $\alpha$ (°) | 90 | 90 | 90 | 90 | 90 |
| $\beta$ (°) | 90 | 94.255(2) | 94.207(2) | 94.184(2) | 90 |
| $\gamma$ (°) | 90 | 90 | 90 | 90 | 90 |
| $V$ (Å$^3$) | 4189.1(13) | 3475.57(12) | 3466.03(15) | 3571.87(14) | 1921.72(9) |
| $Z$ | 4 | 4 | 4 | 4 | 8 |
| $\rho$ (g cm$^{-3}$) | 1.430 | 1.400 | 1.403 | 1.451 | 1.537 |
| $\mu$ (mm$^{-1}$) | 1.231 | 3.123 | 3.131 | 0.819 | 0.515 |
| $\theta$min < 2$\theta$ < $\theta$max | 2.04 < 2$\theta$ < 24.99 | 3.1 < 2$\theta$ < 62.1 | 3.1 < 2$\theta$ < 62.4 | 2.9 < 2$\theta$ < 29.3 | 3.1 < 2$\theta$ < 25.0 |
| Data collected, Uniq. Data, | 4532, 3640 | 11058, 5367 | 11129, 5361 | 46190, 8847 | 5062, 1630 |
| Independent reflections ($R_{int}$) | 1758 (0.068) | 4729 (0.020) | 4872 (0.018) | 7627 (0.033) | 1473 (0.037) |
| $R_1$, $wR_2$ [$I > 2\sigma(I)$], S | 0.0789, 0.2223, 1.06 | 0.0270, 0.0749, 1.03 | 0.0284, 0.0787, 1.03 | 0.0237, 0.0576, 1.06 | 0.0263, 0.0546, 0.96 |

### *4.5. Saturation transfer difference $^1$H NMR experiments*

NMR samples for the saturation transfer difference experiments were prepared in 99.9% $D_2O$ buffer containing 20 mM Tris (98% $D_{11}$), 7 mM $(ND_4)_2SO_4$ (98% $D_8$), 3.5 mM $MgCl_2$ and 0.3 mM DTT (98% $D_{10}$), pD 9. Ligand concentration was 0.4 mM and the protein concentration was 0.004 mM resulting in protein–ligand ratio of 1:100.

The saturation transfer difference NMR experiments [22b] were recorded on Varian 800 MHz spectrometer equipped with cold probe with spectral width of 9058 Hz, 8192 complex data points and 4000–7000 scans. Relaxation delay was set to 10 s. Selective on-resonance irradiation frequency was set to 0.32 ppm with saturation time of 0.4 s. In case of compound **3** saturation time of 2 s was used to improve poor signal to noise ratio in STD spectrum. Selective saturation was achieved by a train of 50 ms Gauss-shaped pulses separated by a 1 ms delay. Off-resonance irradiation frequency for the reference spectrum was applied at 30 ppm. Water suppression was achieved with excitation sculpting [25]. Spectra were zero filled twice and line broadening function of 1 Hz was applied.

## 5. Computational details

Computational modelling of the inhibition effect of the complexes through docking studies, was performed with the grid based version of the MolDock algorithm [26a] as this is implemented in Molegro Virtual Docker software package (www.molegro.com). The three dimensional coordinates of lipoxygenase (LOX) (pdb ID: 1F8N) were obtained from the Protein Data Bank. (www.rcsb.org/pdb). All solvent molecules were removed from the protein

structure. Molecular structures of ligands were obtained by X-ray crystallography. Preceding the docking however, all structures were optimized under the quick PM3 parameterization scheme [26b] to exclude lattice effects non applicable to our theoretical set-up. The default parameters were used regarding charges, bonds order and geometrical flexibility with no other constrains. The docking space was an extensive spherical domain at the centre of the enzyme and the final poses were sorted using the "reranking score" scheme.

## Acknowledgments

This research was carried out in partial fulfillment of the requirements for the Master thesis of G.B. within the graduate program of the Department of Chemistry under the supervision of S.K.H., at the University of Ioannina, Greece.

## Appendix A. Supplementary material

CCDC 820433 (**1**), 820431 (**2**), 820426 (**3a**), 820427 (**3b**), 820430 (**4**), 820429 (**5**), 820432 (**6**) and 820428 $(pmt)_2$ contains the supplementary crystallographic data for this paper. These data can be obtained free of charge from The Cambridge Crystallographic Data Centre via www.ccdc.cam.ac.uk/data_request/cif. Supplementary data associated with this article can be found, in the online version, at doi:10.1016/j.ica.2011.10.024.

## References

[1] T. Tsukihara, H. Aoyama, E. Yamashita, T. Tomizaki, H. Yamaguchi, K. Shinzawa-Itoh, R. Nakashima, R. Yaono, S. Yoshikawa, Science 269 (1995) 1069.
[2] F. Kubowitz, Biochem. Z. 299 (1938) 32.
[3] C.R. Dawson, M.F. Mallette, Adv. Protein Chem. 2 (1945) 179.
[4] (a) B.L. Vallee, W.E.C. Wacker, Proteins 5 (1970) 41. 83, 143;
(b) L. Banci, I. Bertini, F. Cantini, I.C. Felli, L. Gonnelli, N. Hadjiliadis, R. Pierattelli, A. Rosato, P. Voulgaris, Nat. Chem. Biol. 2 (2006) 367.
[5] (a) T. Ottersen, L. Warner, K. Seffh, Inorg. Chem. 13 (1974) 1904;
(b) L.G. Warner, T. Ottersen, K. Seff, Inorg. Chem. 13 (1974) 2819;
(c) C.J. Simmons, M. Lundeen, K. Seff, Inorg. Chem. 18 (1979) 3444;
(d) T. Wallace, J. Org. Chem. 31 (1966) 3071;
(e) P. Kumar, M. Gusain, R. Nagarajan, Inorg. Chem. 50 (2011) 3065.
[6] (a) S.K. Hadjikakou, C.D. Antoniadis, P. Aslanidis, P.J. Cox, A.C. Tsipis, Eur. J. Inorg. Chem. (2005) 1442;
(b) P. Aslanidis, P.J. Cox, P. Karagiannidis, S.K. Hadjikakou, C.D. Antoniadis, Eur. J. Inorg. Chem. (2002) 2216;
(c) P. Karagiannidis, S.K. Hadjikakou, P. Aslanidis, A. Huntas, Inorg. Chim. Acta 178 (1990) 27;
(d) S.K. Hadjikakou, P. Aslanidis, P.D. Akrivos, P. Karagiannidis, B. Kojic-Prodic, M. Luic, Inorg. Chim. Acta 197 (1992) 31;
(e) P. Aslanidis, S.K. Hadjikakou, P. Karagiannidis, B. Kojic-Prodic, M. Luic, Polyhedron 12 (1994) 3119.
[7] (a) P.D. Akrivos, S.K. Hadjikakou, P. Karagiannidis, D. Mentzafos, A. Terzis, Inorg. Chim. Acta 206 (1993) 163;
(b) S.K. Hadjikakou, P.D. Akrivos, P. Karagiannidis, D. Mentzafos, A. Terzis, Inorg. Chim. Acta 210 (1993) 27.
[8] (a) B.-J. Liaw, T.S. Lobana, Y.-W. Lin, J.-C. Wang, C.W. Liu, Inorg. Chem. 44 (2005) 9921;
(b) J.T. Gill, J.J. Mayerle, P.S. Welcker, D.F. Lewis, D.A. Ucko, D.J. Barton, D. Stowens, S.J. Lippard, Inorg. Chem. 15 (1976) 1155.
[9] S.S. Batsanov, Inorg. Mater. 37 (2001) 871.
[10] (a) C.-H. Li, S.C.F. Kui, I.H.T. Sham, S.S.-Y. Chui, C.-M. Che, Eur. J. Inorg. Chem. (2008) 2421;
(b) P.C. Ford, E. Cariati, J. Bourassa, Chem. Rev. 99 (1999) 3625;
(c) V.W.-W. Yam, K.K.-W. Lo, Chem. Soc. Rev. 28 (1999) 323.
[11] (a) B. Samuelsson, S.E. Dahlen, J. Lindgren, C.A. Rouzer, C.N. Serhan, Science 237 (1987) 1171;
(b) M.J. Knapp, J.P. Klinman, Biochemistry 42 (2003) 11466;
(c) X.-Z. Ding, C.A. Kuszynski, T.H. El-Metwally, T.E. Adrian, Biochem. Biophys. Res. Commun. 266 (1999) 392;
(d) G.P. Pidgeon, J. Lysaght, S. Krishnamoorthy, J.V. Reynolds, K. O'Byrne, D. Nie, K.V. Honn, Cancer Metastasis Rev. 26 (2007) 503.
[12] (a) D. Li, W.-J. Shi, T. Wu, S.W. Ng, Acta Crystallogr., Sect. E: Struct. Rep. Online 60 (2004) m776;
(b) T.S. Lobana, P. Kaur, A. Castineiras, P. Turner, T.W. Failes, Struct. Chem. 19 (2008) 727;
(c) C.-X. Ruan, W.-J. Shi, Acta Crystallogr., Sect. E: Struct. Rep. Online 63 (2007) m2412;
(d) P. Aslanidis, P. Karagiannidis, P.D. Akrivos, B. Krebs, M. Lage, Inorg. Chim. Acta 254 (1997) 277.
[13] (a) S. Furberg, J. Solbakk, Acta Chem. Scand. 27 (1973) 2536;
(b) G.B. Jensen, G. Smith, D.S. Sagatys, P.C. Healy, J.M. White, Acta Crystallogr., Sect. E: Struct. Rep. Online 60 (2004) o2438.
[14] P. Strauch, W. Dietzsch, L. Golic, Z. Anorg. Allg. Chem. 623 (1997) 129.
[15] (a) S. Sculfort, P. Braunstein, Chem. Soc. Rev. 40 (2011) 2741;
(b) P. Pyykko, Chem. Rev. 97 (1997) 597.
[16] (a) S.M. Nelson, F.S. Esho, M.G.B. Drew, Chem. Commun. (1981) 388;
(b) I.F. Taylor Junior, M.S. Weininger, E.L. Amma, Inorg. Chem. 13 (1974) 2835;
(c) H.-G. Zhu, H. Cai, Y. Xu, Z. Yu, X.-Z. You, C.H.L. Kennard, J. Coord. Chem. 49 (1999) 75;
(d) G.-H. Zhang, N.-Z. Wu, X.-L. Jin, P. Wang, H.-Y. Guo, Chin. J. Chem. 21 (2003) 40;
(e) M. Belicchi-Ferrari, F. Bisceglie, E. Buluggiu, G. Pelosi, P. Tarasconi, Polyhedron 28 (2009) 1160;
(f) R.K. Chadha, R. Kumar, D.G. Tuck, Can. J. Chem. 65 (1987) 1336;
(g) E.S. Raper, J.R. Creighton, J.D. Wilson, W. Clegg, A. Milne, Inorg. Chim. Acta 149 (1988) 265;
(h) H. Xu, J.H.K. Yip, Inorg. Chem. 42 (2003) 4492.
[17] (a) M. Spescha, G. Rihs, Helv. Chim. Acta 76 (1993) 1219;
(b) S. Schneider, J.A.S. Roberts, M.R. Salata, T.J. Marks, Angew. Chem., Int. Ed. 45 (2006) 1733;
(c) Y. Agnus, R. Louis, R. Weiss, Chem. Commun. (1980) 867;
(d) R. Castro, M.L. Duran, J.A. Garcia-Vazquez, J. Romero, A. Sousa, E.E. Castellano, J. Zukerman-Schpector, J. Chem. Soc., Dalton Trans. (1992) 2559;
(e) K. Johnson, J.W. Steed, J. Chem. Soc., Dalton Trans. (1998) 2601;
(f) Y.-D. Chen, L.-Y. Zhang, Y.-H. Qin, Z.-N. Chen, Inorg. Chem. 44 (2005) 6456; J. Lang, K. Tatsumi, K. Yu, Polyhedron 15 (1996) 2127.
[18] K. Lazarou, B. Bednarz, M. Kubicki, I.I. Verginadis, K. Charalabopoulos, N. Kourkoumelis, S.K. Hadjikakou, Inorg. Chim. Acta 363 (2010) 763.
[19] (a) P.F. Barron, J.C. Dyason, P.C. Healy, L.M. Engelhardt, C. Pakawatchai, V.A. Patrick, A.H. White, J. Chem Soc., Dalton Trans. (1987) 1099;
(b) K. Folting, J. Huffman, W. Mahoney, J.M. Stryker, K.G. Caulton, Acta Crystallogr., Sect. C: Cryst. Struct. Commun. 43 (1987) 1490;
(c) T. Krauter, B. Neumuller, Polyhedron 15 (1996) 2851;
(d) V.G. Albano, P. Bellon, M. Sansoni, J. Chem. Soc., A (1971) 2420;
(e) A. Machado, G.N. ManzonideOliveira, H. Fenner, R.A. Burrow, Acta Crystallogr., Sect. C: Cryst. Struct. Commun. 64 (2008) m233.
[20] M. Kubicki, S.K. Hadjikakou, M.N. Xanthopoulou, Polyhedron 20 (2001) 2179.
[21] I. Reva, L. Lapinski, M.J. Nowak, Chem. Phys. Lett. 467 (2008) 97.
[22] (a) M.N. Xanthopoulou, S.K. Hadjikakou, N. Hadjiliadis, M. Kubicki, S. Karkabounas, K. Charalabopoulos, N. Kourkoumelis, T. Bakas, J. Organomet. Chem. 691 (2006) 1780;
(b) M. Mayer, B. Meyer, J. Am. Chem. Soc. 123 (2001) 6108.
[23] (a) M.N. Xanthopoulou, S.K. Hadjikakou, N. Hadjiliadis, E.R. Milaeva, J.A. Gracheva, V.-Y. Tyurin, N. Kourkoumelis, K.C. Christoforidis, A.K. Metsios, S. Karkabounas, K. Charalabopoulos, Eur. J. Med. Chem. 43 (2008) 327;
(b) I. Ozturk, S. Filimonova, S.K. Hadjikakou, N. Kourkoumelis, V. Dokorou, M.J. Manos, A.J. Tasiopoulos, M.M. Barsan, I.S. Butler, E.R. Milaeva, J. Balzarini, N. Hadjiliadis, Inorg. Chem. 49 (2010) 488;
(c) V.I. Balas, S.K. Hadjikakou, N. Hadjiliadis, N. Kourkoumelis, M.E. Light, M. Hursthouse, A.K. Metsios, S. Karkabounas, Bioinorg. Chem. Appl. (2008) Article ID 654137.
[24] (a) Oxford Diffraction, CRYSALIS CCD and CRYSALIS RED, version p171.29.2, Oxford Diffraction Ltd., Abingdon, Oxford, England, (2006);
(b) CrysAlis RED, Oxford Diffraction Ltd., Version 1.171.31.5 (release 28-08-2006 CrysAlis171.NET);
(c) G.M. Sheldrick, SHELXS97 Program for Crystal Structure solution, University of Goettingen, Germany, (1997);
(d) G.M. Sheldrick, Acta Crystallogr., Sect. A46 (1990) 467;
(e) G.M. Sheldrick, SHELXL-97, Program for the Refinement of Crystal Structures, University of Göttingen, Göttingen, Germany, (1997).
[25] (a) H.L. Hwang, A.J. Shaka, J. Magn. Reson. Ser. A 112 (1995) 275;
(b) C. Dalvit, J. Biomol. NMR 11 (1998) 437.
[26] (a) R. Thomsen, M.H. Christensen, J. Med. Chem. 49 (2006) 3315;
(b) J.J.P. Stewart, J. Comput. Chem. 10 (1989) 210.